Inorganica Chimica Acta, 140 (1987) 215–230

Determination of Lanthanides and of U and Th in Geological Samples*

R. GIJBELS

University of Antwerp (U.I.A.), Department of Chemistry, B-2610 Antwerp–Wilrijk, Belgium

Abstract

A review is presented on analytical techniques which are frequently used to determine the lanthanides and U and Th in geological samples. Instrumental neutron activation analysis followed by high-resolution gamma-ray spectrometry using conventional coaxial and planar germanium detectors is applicable to most practical problems. Radiochemical neutron activation analysis allows the analysis of very small samples, or samples containing the lanthanides at the sub-ppm to ppb level; the latter elements are usually separated from the remainder as a group. Various types of mass spectrometry, combined or not with isotope dilution techniques (e.g., thermal ionization, spark source and inductively coupled plasma mass spectrometry) will be discussed with regard to sensitivity, accuracy, interferences and cost-effectiveness. Of the microbeam methods for the *in situ* determination of the lanthanides in individual mineral crystals, secondary ion mass spectrometry (ion microprobe mass analysis) is presently the only method with sufficient sensitivity. Delayed neutron counting is a suitable method for determining U and Th in large series of bulk samples; the distribution of these elements can be studied using the fission track technique.

Introduction

The abundances of rare earth elements (REE) in natural materials have become an important geochemical tool. Geochemically, the term 'rare earth' is best restricted to mean lanthanides plus yttrium [1]. REE comprise a unique coherent group: wherever one rare earth appears, all others are present as well. The group is coherent because under most natural conditions all members share a common (3+) oxidation state, with anomalous behaviour occurring under some conditions for Ce (4+) and Eu (2+). Natural materials differ substantially from each other in concentrations of the REE as a group and in abundances of individual REE relative to each other. In most natural situations, chemical separations within the group occur as a smooth function of atomic number. This makes it possible to find genetic relationships among diverse natural materials and to determine by what processes some natural materials are formed [1].

From the geometrical point of view, the REE are 'dispersed' (not so 'rare') elements, *i.e.*, they are spread among many common materials, rather than concentrated into a select few. They are 'lithophile', *i.e.* when allowed to distribute themselves among common silicate, metal and sulphide phases, they overwhelmingly enter the silicates. However, during igneous processes the REE tend to remain in the liquid phase as most minerals are not able to incorporate them. The minerals that do take up REE in their structures will generally show a preference for either light (LREE) or heavy (HREE) REE, depending on the nature of the ionic positions available for substitution. This is a consequence of the regular decrease in ionic radii for the trivalent REE from La to Lu (the so-called lanthanide contraction).

The use of the REE as a geochemical tool began in the early 1960s with the development of techniques for their analysis by neutron activation, followed by methods of isotope dilution mass spectrometry. These techniques provided measurements of sufficient accuracy on common, but chemically complex, natural materials for which the potential use of REE distributions could be recognized and put to use. Summaries of early work are given by Haskin *et al.* [2], Herrmann [3] and Haskin and Korotev [4].

When comparing the REE contents of different rocks or minerals, one generally normalizes the concentrations of the individual REE to their abundance in chondrites (the meteorites that best represent the composition of the non-volatile fraction of solar system material). This is done to take into account the fact that elements with even atomic numbers are more abundant than their neighbours with odd atomic numbers (Oddo–Harkins effect), a consequence of nuclear stability. This normalization results in REE patterns (normalized concentration *versus* atomic number) that are smooth, except for occa-

*Paper presented at the Second International Conference on the Basic and Applied Chemistry of f-Transition (Lanthanide and Actinide) and Related Elements (2nd ICLA), Lisbon, Portugal, April 6–10, 1987.

0020-1693/87/$3.50

sional anomalies for Eu and Ce (because of their sometimes differing oxidation states) and for Eu and Yb (the two most volatile REE that are sometimes depleted in the refractory Ca–Al-rich inclusions present in carbonaceous chondrites). General reviews of REE geochemistry have been written by Haskin and Paster [1], Hanson [5] and Henderson [6].

We will first discuss the most widely used analytical methods for the REE, and thereafter recently developed techniques. We will not only address the analysis of bulk samples but also *in situ* microanalysis of the REE. Some attention will also be paid to other elements, in particular U and Th.

Neutron Activation Analysis (NAA)

NAA has been applied to cosmochemical and geochemical problems from the time the first nuclear research reactors became available in the late 1940s [7]. Undoubtedly the most significant contribution of early NAA to modern geo- and cosmochemistry was the work dealing with the distribution of the REE in meteorites, rocks and sediments [8–10]. The methodology included dissolution of the sample, after neutron irradiation, in the presence of inactive carriers, separation of the individual REE by ion exchange chromatography, whole γ or β counting of the individual pure fractions, and determining the yield of the radiochemical separation (e.g., by titration) to correct for losses during the chemical procedure.

Instrumental Neutron Activation Analysis

With the introduction of high-resolution Ge(Li) γ-ray detectors many trace elements, including the REE, could be determined simultaneously without any chemical separations in a wide variety of rocks and minerals by 'instrumental' NAA, or INAA [11, 12]. INAA rapidly became a standard technique for trace element analysis of silicate materials; this is also due to the favourable nuclear characteristics of most of the major elements in silicates (low neutron activation cross-sections, short half-lives and/or low γ-ray abundances in the nuclear decay). Now it is hard to find a single issue of the major geo- and cosmochemical journals without a paper dealing with data obtained by INAA.

Gordon *et al.* [11] were the first to fully demonstrate the potentialities of INAA employing large Ge(Li) detectors for multi-element analysis of a wide variety of silicate rocks. Through a combination of two irradiations in a thermal neutron flux and countings at various intervals after irradiation, they were able to determine about 20 elements, many of them present at 0.1–100 ppm concentration levels. It was soon realized that the accuracy and precision for a number of trace elements, including the lanthanides and uranium, could be significantly improved by γ-ray spectrometry employing low-energy photon detectors (LEPD) [12] and selective activation with epithermal neutrons [13].

As compared to large-volume Ge(Li) detectors, the extra high resolution, thin Ge(Li) or hyperpure Ge detectors greatly reduce peak overlapping and greatly enhance peak-to-background ratios in the 50–400 keV energy range, resulting in much better data for radionuclides having their most intense (or only) photopeaks in this range. This is the case for many lanthanides, as a result of their low-lying rotation energy levels, caused by collective motion of their non-spherical nuclei. However, because of the low detection efficiency for higher-energy photons, LEPDs cannot be used to determine the full range of elements. Large Ge(Li) detectors and small LEPDs should rather be considered as complementary. Tables I and II summarize some relevant properties of useful radionuclides observable with conventional Ge(Li) and low-energy photon detectors in reactor neutron-irradiated silicate rocks. It can be seen that the REE, U and Th belong to the group of elements with favourable characteristics.

By irradiating silicates under a 0.5–1 mm cadmium cover, the thermal neutron flux (up to *ca.* 0.5 eV) is reduced by a factor of about 5000, resulting in an enhanced relative sensitivity of elements with high resonance integrals relative to Na, Sc, Cr, Fe, Co, La and Eu. The latter are mainly activated by thermal neutrons, and often dominate the γ-ray spectrum of thermal neutron-activated silicate rocks by a high Compton continuum.

Table III summarizes the results of an evaluation of the relative merits of thermal and epithermal NAA using large Ge(Li) and LEPD detectors [14]. ENAA is especially suited for basaltic rocks that have relatively high Sc, Cr, Fe and Co concentrations.

Methodological approaches have not changed dramatically since the early 1970s. Nevertheless, significant progress has been made through a better understanding of factors controlling accuracy and precision, the steady improvement of nuclear instrumentation, the availability of computer-based counting systems, and the development of sophisticated computer programs for data reduction (see ref. 7 and refs. therein).

Table IV shows a typical irradiation/counting scheme for the determination of short- and long-lived radionuclides. The completion of a 'long' cycle takes 3–4 weeks; the method is thus not particularly fast. However, up to 20 samples can be irradiated simultaneously, and countings from several irradiations can be carried out concurrently. The capacity of a well-equipped laboratory is 300–600 samples per year [7]. The determination of dysprosium requires a separate, short irradiation (5 min) and a counting after a 30–60 min cooling time. INAA does not only

TABLE I. Properties of Analytically Useful Radionuclides Observable with a 'Conventional' Ge(Li) Detector in Reactor-irradiated Silicate Rocks

Element	Product radionuclide (half-life)	Best time after irradiation for counting	Best photopeaks used in determination (keV) (absolute intensity (%))	Interference or remark[a]
Na	^{24}Na (15.0 h)	1 day	1368.65 (100)	
			1731.9 (DE)	
K	^{42}K (12.4 h)	1 day	1524.7 (18)	
Rb	^{86}Rb (18.66 d)	2–4 weeks	1076.6 (8.8)	^{59}Fe 1291.58
				Compton edge
Cs	^{134}Cs (2.05 y)	few months	604.7 (98)	*^{124}Sb 602.7*
			795.8 (88)	
Ba	^{131}Ba (12 d)	2–4 weeks	216.0 (19)	*^{160}Tb 215.65*
			373.2 (13)	^{233}Pa 375.4
			496.3 (45)	
La	^{140}La (40.23 h)	4–5 days	328.7 (21)	^{140}La 487.0
				Compton edge
			487.0 (46)	^{181}Hf 482.0
			815.8 (24)	
			1596.2 (97)	
Ce	^{141}Ce (32.53 d)	2–4 weeks	145.5 (49)	*^{59}Fe 142.5*; ^{175}Yb 144.7; ^{233}Pa 145.4
Nd	^{147}Nd (10.99 d)	2–4 weeks	91.0 (27)	^{131}Ba 92.3
				^{182}Ta 100.1 + 84.7
				^{170}Tm 84.3
				^{169}Yb 84.2 + 93.6
				^{175}Hf 89.6
				^{153}Sm 89.5 + 97.5 + 103.2
				^{160}Tb 87.2 + 93.9
				^{233}Pa 86.8 + 103.8 + U Kα_1 (98.5) + U Kα_2 (94.7)
				^{153}Gd 97.5 + 103.2
			531.0 (13)	
Sm	^{153}Sm (46.5 h)	4–5 days	103.23 (27)	^{153}Gd 103.23
				^{233}Pa U X-rays
Eu	^{152}Eu (13 y)	few months	121.83 (29.4)	*^{131}Ba 123.73*
				^{154}Eu 122.91
			244.54 (7.6)	^{154}Eu 247.73
				^{131}Ba 246.8
			779.08 (14.5)	
			1408.11 (22.9)	
	^{154}Eu (8.6 y)	few months	723.29 (21)	*^{95}Zr 724.24*
			1274.53 (37)	^{160}Tb 1271.87
Gd	^{153}Gd (241.5 d)	few months	97.43 (51.5)	^{233}Pa U X-rays
			103.18 (39)	^{182}Ta 100.10
Tb	^{160}Tb (72.3 d)	few months	298.58 (26.3)	*^{233}Pa 300.2*
			962.08 (12.6)	*^{152}Eu 964.21*
			966.10 (27.6)	
Dy	^{165}Dy (2.35 h)	few hours	94.7 (3.7)	^{233}Pa U X-rays
				^{233}Th Pa Kα_1
Tm	^{170}Tm (129 d)	few months	84.26 (3.4)	^{160}Tb 86.79
				^{182}Ta 84.68
				^{233}Pa 86.59
Yb	^{169}Yb (31 d)	1 month	63.5 (57.3)	*^{182}Ta 65.72*
			177.0 (20.2)	^{182}Ta 179.39
			197.8 (34.9)	*^{160}Tb 197*
				^{182}Ta 198
	^{175}Yb (4.19 d)	1–2 weeks	282.6 (3.7)	
			396.1 (6.0)	*^{160}Tb 392.51*
				^{233}Pa 399.6

(continued)

TABLE I. *(continued)*

Element	Product radionuclide (half-life)	Best time after irradiation for counting	Best photopeaks used in determination (keV) (absolute intensity (%))	Interference or remark[a]
Lu	^{177}Lu (6.71 d)	2 weeks	208.36 (7.5)	^{131}Ba 216.00 ^{160}Tb 215.65 ^{239}Np 209.73
Th	^{233}Pa (27.0 d)	2–4 weeks	311.9 (34.0) 415.9 (1.5)	^{169}*Yb 307.5* ^{152}Eu 411.06
Zr	^{95}Zr (65.5 d)	few months	724.24 (43.1) 756.87 (54.9)	^{154}Eu 723.29 ^{154}Eu 756.78
	^{95}Nb (35.1 d)		765.80 (100)	^{160}Tb 765.19
Hf	^{181}Hf (42.4 d)	1 month	133.02 (40) 136.25 (6) 136.86 (1.7)	^{131}Ba 133.54 ^{169}Yb 130.7
Ta	^{182}Ta (115 d)	few months	67.75 (41.7)	^{169}*Yb 63.5* ^{153}Gd 70
			100.10 (14.2)	^{233}*Pa 94–98* ^{153}Gd 97.43 103.18
			1121.22 (35.0)	
Sb	^{122}Sb (2.72 d)	1 week	564.0 (66.3)	^{134}Cs 563.2 569.33
	^{124}Sb (60.20 d)	few months	1691.0 (50)	
Mn	^{56}Mn (2.582 h)	few hours	846.78 (99.0)	^{152m}Eu 841.39 (^{27}Mg 844.0)
			1810.96 (29.7)	
Co	^{60}Co (5.272 y)	few months	1173.226 (99.9) 1332.483 (100.0)	^{160}Tb 1178.12
Fe	^{59}Fe (44.6 d)	few months	1099.27 (56) 1291.58 (44)	^{152}Eu 1292.62 ^{182}Ta 1289.13
Sc	^{46}Sc (83.8 d)	few months	889.25 (100.0)	^{46}Sc 1120.50 Compton edge
			1120.50 (100.0)	^{182}*Ta 1121.22* ^{152}Eu 1112.20
Cr	^{51}Cr (27.71 d)	1 month	320.08 (9)	^{233}Pa 311.9 ^{147}Nd 319.4

[a]Prominent peaks which interfere with the analytical peak listed in column 4 are italicized in column 5. In other cases the interference is usually negligible or can be eliminated by suitable cooling time; e.g., 9.6 min ^{27}Mg (844.0) interference on 2.582 h ^{56}Mn (846.78 keV).

yield information on REE in a wide variety of silicate rock types (except ultrabasic rocks), but also on a number of other elements: major, minor and trace elements, including Th and U, see also Tables I and II.

Powdered rock or mineral samples of 100–500 mg are suitable for most concentration levels, but less material can be used if the sample is in short supply. The required amount of sample obviously also depends on the available neutron flux.

By adding a little polyethylene wax or graphite, the powdered sample can easily be pelletized, resulting in well-defined irradiation and counting geometry, which is especially important to avoid errors when using the small low-energy photon detectors. In the conventional standardization methods, an appropriate amount of a stock solution of the REE is evaporated on filter paper or on high purity silica. Alternatively, in-house standard rocks can be used, which have been standardized against international standard rocks, e.g. from the U.S. Geological Survey [15].

With careful standardization, results of INAA can be accurate to within a few percent. Sources of errors in INAA have been discussed in detail by De Soete *et al.* [16], and some of them are relevant in the present context: special attention is drawn to the corrections for dead-time losses in the counting of short-lived radionuclides [17].

To illustrate the performance of INAA for common silicate materials, Table V lists the mean values of six replicate analyses of I.A.E.A. reference sample Soil-5 [18]. The averages calculated from all available data [19] are shown for comparison.

TABLE II. Properties of Analytically Useful Radionuclides Observable with Low-energy Photon Ge(Li) of Ge Detectors in Reactor-neutron-irradiated Silicate Rocks [12]

Element	Product radionuclide (half-life)	Irrad. and decay time[a]	Best photopeak used for analysis (keV) (absolute intensity (%))	Interference or remark[b]
La	^{140}La (40.23 h)	(a)	328.7 (21)	^{194}Ir[c]
Ce	^{141}Ce (32.53 d)	(b)	145.4 (49)	sepd. from ^{59}Fe 142.5 count after decay of ^{175}Yb 144.7
Nd	^{147}Nd (10.99 d)	(b)	91.0 (27)	
Sm	^{153}Sm (46.5 h)	(a)	69.68 (4.6)	*Au Kα$_1$ 68.8*
			103.23 (27)	^{239}Np (Pu Kα$_1$) 103.6
Eu	^{152}Eu (13 y)	(b)	121.83 (29.4)	^{147}Nd 120.5
			244.54 (7.6)	
Gd	^{153}Gd (241.5 d)	(b)	97.43 (51.5)	*^{233}Pa (U Kα$_1$) 98.5*
				^{153}Sm 97.4
			103.18 (39.0)	*^{233}Pa 103.8*
				^{153}Sm 103.2
Tb	^{160}Tb (72.3 d)	(b)	86.8 (12.0)	*^{233}Pa 86.6*
			298.6 (26.3)	*^{233}Pa 299.9*
Dy	^{165}Dy (2.35 h)	(c)	94.7 (3.7)	
			47.5 (Ho Kα$_1$)	^{152m_1}Eu (Sm Kβ′$_1$)
			46.7 (Ho Kα$_2$)	45.4 + 46.6
Ho	^{166}Ho (26.8 h)	(a)	80.57 (<0.1)	Au Kβ′$_2$ 80.2 + ?
Tm	^{170}Tm (129 d)	(b)	84.26 (3.4)	*^{182}Ta 84.7*
				^{169}Yb 84.2
Yb	^{169}Yb (31 d)	(b)	63.5 (57.3)	^{175}Hf (Lu Kβ′$_2$) 62.9
			130.7 (11.2)	^{140}La 131.0
			177.0 (20.2)	
			50.7 (Tm Kα$_1$)	^{170}Tm (Yb Kα$_2$) 51.3
			49.7 (Tm Kα$_2$)	^{152}Eu (Gd Kβ′$_2$) 50.0
Lu	^{177}Lu (6.71 d)	(b)	208.36 (7.5)	^{169}Yb 207.4
				^{239}Np 209.8
Ta	^{182}Ta (115 d)	(b)	67.75 (41.7)	^{182}Ta (W Kβ′$_1$) 67.2
				Au Kα$_2$ 67.0
				^{181}Hf (Ta Kβ′$_2$) 67.0
			100.10 (14.2)	^{233}Pa (U Kα$_1$) 98.5
			152.44 (7.2)	
			222.11 (8.0)	
			59.3 (W Kα$_1$)	^{169}Yb (Tm Kβ′$_2$) 59.0 (small correction)
U	^{239}Np (2.350 d)	(a)	106.13 (21.9)	^{155}Eu 105.4[d]
Th	^{233}Pa (27.0 d)	(b)	311.9 (34.0)	
			98.4 (U Kα$_1$)	*^{153}Gd 97.5*
				^{239}Np (Pu Kα$_2$) 99.5
				^{182}Ta 100.1
			94.7 (U Kα$_2$)	*^{169}Yb 93.6*
				^{160}Tb 93.9
Cr	^{51}Cr (27.71 d)	(b)	320.08 (9)	^{147}Nd 319.4
Fe	^{59}Fe (44.6 d)	(b)	142.45 (0.8)	
			192.23 (2.5)	
Ba	^{139}Ba (83.3 min)	(c)	165.8 (21.7)	
	^{131}Ba (11.7 d)	(b)	123.73 (26)	*^{154}Eu 123.3*
			216.0 (19)	*^{160}Tb 215.6*
Hf	^{181}Hf (42.4 d)	(b)	133.02 (40.0)	
			136.25 (6.0)	^{177}Lu 136.7
			136.86 (1.7)	

[a]Irradiation and decay time: (a) 6 h irradiation, 7 d cooling time, 30 min counting time; (b) 6 h irradiation, 15–35 d cooling time, 2–8 h counting time; (c) 5 min irradiation, 1 h cooling time, 30 min counting time. [b]Prominent peaks which interfere with the analytical peak listed in column 4 are italicized in column 5. In other cases the interference is usually negligible or can be eliminated by suitable cooling time; Au K X-rays are produced if the LEPD has a gold coating on the top. [c]This occurs in special samples only, e.g., in irradiated diamonds. [d]Formed by reactions ^{153}Eu(n, γ)(n, γ)^{155}Eu and/or ^{154}Sm(n, γ)(β^-)^{155}Eu.

TABLE III. A Comparison of the Utility of Various Irradiation and Counting Procedures for Instrumental NAA of Common Silicate Rocks (Long-lived Radionuclides Only)[a]

Element	Basaltic rocks				Granitic rocks			
	Thermal		Epithermal		Thermal		Epithermal	
	Ge(Li)	LEPD	Ge(Li)	LEPD	Ge(Li)	LEPD	Ge(Li)	LEPD
Sc	G*		S		G*		S–M	
Cr	G*	G	S–M		M*		I	
Fe	G*		S		G*		S	
Co	G*		S		S*		S	
Ni	M–I		S–M*		I		M–I*	
Zn	M		M*		M		M*	
Se	I	I	I	I	I	I	I	M–I
Rb	M–I		S–M*		S–M		G*	
Sr	I		S–M*		M		S*	
Zr	M–I		M–I		M		M	
Mo	I	I	I	M–I*	I	I	I	M*
Sb	S–M		S*		S–M		S*	
Cs	M		S–M*		S–M		G*	
Ba	M–I	M–I	S–M	S*	S–M	S–M	S	S*
La	G*		S		G*		S	
Ce	S	G*	S	S	S	G*	S	S
Nd	M	G*	I	S	M	G*	I	S
Sm	S	G*	S	G	S	G*	S	G
Eu	G*	G	M	S	G*	G	S–M	S
Gd	I	M	I	M*	I	M	I	M*
Tb	M	G	S	S	S	S	G*	S
Tm	I	M	I	M–S*	I	S–M	I	S*
Yb	S–M	S	S–M	S*	S	S	S	S*
Lu	S–M	S*	M	M	S	S*	M	M
Hf	S–M	S	S	G*	G	S	G	G*
Ta	S–M	S	G*	G	S	G	G*	G
Th	S–M	S	G*	G	S	G	G*	G
U	I	S–M	S	S*	I	S	G	G*

[a]From Baedecker *et al.* [14] with modifications. G = good; S = satisfactory; M = marginal; I = impossible. * = best method.

TABLE IV. Sequential Irradiation/Counting Scheme for Instrumental NAA of Common Silicate Rocks

	t_{irr}	t_{delay}	Radionuclides measured	
			Ge(Li)	LEPD
(A)	20 s	15 s	^{46m}Sc, ^{179m}Hf	
(B)	5 min	3–5 min	^{27}Mg, ^{28}Al, ^{49}Ca, ^{51}Ti, ^{52}V	^{60m}Co, ^{155}Sm, ^{239}U
		30–60 min	^{24}Na, ^{56}Mn	^{139}Ba, ^{152m}Eu, ^{165}Dy
(C)	⩾1 h	7 d	^{24}Na, ^{46}Sc, ^{51}Cr, ^{59}Fe, ^{60}Co, ^{131}Ba, ^{140}La, ^{153}Sm, ^{152}Eu, ^{175}Yb, ^{177}Lu	^{51}Cr, ^{59}Fe, ^{131}Ba, ^{140}La, ^{141}Ce, ^{147}Nd, ^{153}Sm, ^{152}Eu, ^{166}Ho, ^{169}Yb, ^{177}Lu, $^{239}Np(U)$
		15–30 d	^{46}Sc, ^{51}Cr, ^{59}Fe, $^{58}Co(Ni)$, ^{60}Co, ^{65}Zn, ^{86}Rb, ^{85}Sr, ^{95}Zr, ^{124}Sb, ^{134}Cs, ^{131}Ba, ^{152}Eu, ^{160}Tb, ^{181}Hf, ^{182}Ta, $^{233}Pa(Th)$	^{51}Cr, ^{59}Fe, ^{131}Ba, ^{141}Ce, ^{147}Nd, ^{152}Eu, ^{153}Gd, ^{160}Tb, ^{170}Tm, ^{169}Yb, ^{181}Hf, ^{182}Ta, $^{233}Pa(Th)$

Delayed Neutron Counting for Uranium and Thorium

Delayed neutron counting is a specific nuclear method for determining uranium and thorium. If a nuclide having $Z>90$ (e.g., isotopes of thorium, uranium, plutonium and other transuranic elements) undergoes fission, some of the fission-product nuclides decay by β-emission, with half-lives in the range 1–60 s, to highly excited states of daughter nuclei which, in their turn, decay by emission of a neutron. These neutrons are emitted almost instanta-

TABLE V. Precision and Accuracy of INAA, Illustrated with Results for I.A.E.A. Soil-5 [18]

Element	Mean[a]	Reported [19]
Ti	0.52 ± 0.04%	(0.47)
Al	8.10 ± 0.40%	8.19 ± 0.28
Fe	4.85 ± 0.10%	4.45 ± 0.19
Mn	0.090 ± 0.006%	0.085 ± 0.004
Mg	1.2 ± 0.4%	(1.5)
Ca	2.5 ± 0.2%	(2.2)
Na	1.76 ± 0.2%	1.92 ± 0.11
K	1.90 ± 0.10%	1.86 ± 0.11
Sc	15.5 ± 0.3 ppm	14.8 ± 0.66
V	130 ± 10 ppm	(150)
Cr	38 ± 2 ppm	30 ± 3
Co	14.2 ± 0.3 ppm	14.8 ± 0.76
Ni	< 10 ppm	(13)
Zn	350 ± 20 ppm	368 ± 8.2
Sb	14.8 ± 0.8 ppm	14.3 ± 2.2
Rb	120 ± 10 ppm	138 ± 7
Cs	63.0 ± 2 ppm	57 ± 3
Ba	530 ± 30 ppm	561 ± 53
Sr	340 ± 20 ppm	(330)
La	27.3 ± 1.0 ppm	28.1 ± 1.5
Ce	58 ± 2 ppm	60 ± 3
Nd	32 ± 3 ppm	30 ± 2
Sm	5.60 ± 0.20 ppm	5.42 ± 0.40
Eu	1.20 ± 0.10 ppm	1.18 ± 0.08
Tb	0.70 ± 0.03 ppm	0.67 ± 0.08
Dy	4.0 ± 0.3 ppm	4.0 ± 1.0
Yb	2.4 ± 0.10 ppm	2.24 ± 0.20
Lu	0.36 ± 0.02 ppm	0.34 ± 0.044
Zr	220 ± 20 ppm	(220)
Hf	6.0 ± 0.2 ppm	6.3 ± 0.30
Ta	0.81 ± 0.02 ppm	0.76 ± 0.06
Th	11.0 ± 0.80 ppm	11.3 ± 0.73

[a]Mean ± 1 standard deviation of six replicate analyses.

neously after the precursor nuclide has emitted a β-particle, and consequently they exhibit an apparent half-life in their emission which coincides practically with that of the precursor nuclide. These neutrons are known as delayed neutrons, in contrast to those neutrons which are emitted promptly during the process of fission. In order to induce fission, samples containing uranium and thorium are exposed to reactor neutrons. ^{235}U gives fission with slow neutrons; ^{232}Th and ^{238}U with fast neutrons. If two determinations are made for each sample, one in a mixed (fast and slow) neutron flux, and one with the slow neutrons screened out by a cadmium shield, both uranium and thorium may be determined. A serious interference to the determination of Th is the neutron emission by 4.2-s ^{17}N produced by the reaction $^{17}O(n, p)^{17}N$.

Delayed neutron emission from irradiated samples can be measured in a paraffin-moderated BF_3 counter assembly of roughly 4π geometry. Assuming an irradiation time of 60 s at a thermal neutron flux of 5×10^{12} cm^{-2} s^{-1}, a delay time of 20 s and a counting time of 60 s, 1 μg of natural uranium gives 200–400 counts in such a set-up, for a counter background of 5–25 cpm. If the sample weight is *ca.* 20 g, uranium contents of 0.1 ppm can be determined with a standard deviation of ±5%. This shows that the method is both fast and sensitive. For thorium, the technique is less sensitive by more than an order of magnitude. An extensive study of delayed neutron counting was made by Amiel [20], including geological samples, by Dyer *et al.* [21] and by Gale [22].

Due to the short half-lives, an elaborate and costly pneumatic transfer system is required. However, because of the fast analysis turnout, the price per analysis can be quite favourable in routine analysis. The method is applied mainly to the analysis of large series of samples (500–10 000 samples per year) for uranium prospection [23, 24].

The state of the art of this field has been recently discussed in refs. 23–25.

Nuclear Track Counting

Some elements, such as uranium and thorium [26–30] can be determined by fission track counting after irradiation of the sample in a thermal and epithermal or fast neutron flux. The sample is pressed against a dielectric detector in the form of a foil and irradiated; polycarbonate foils ('Lexan', 'Makrofol') or mica detectors are commonly used to catch the recoiling fission fragments. The radiation damage produced by fission fragments can afterwards be observed by etching the foil with a suitable reagent. The nuclear tracks have a characteristic form and can be counted under a microscope. The counting can, however, also be performed with automatic scanning devices. It is obvious that standardization can be carried out by simultaneously irradiating a sample with a known U or Th content.

A surprisingly simple and inexpensive technique for counting tracks in very thin foils (thickness less than the range of the fission fragments) has been developed by Cross and Tommasino [31] and is known as 'spark counting'; see also, for instance, Johnson *et al.* [32].

The determination of uranium and thorium by the fission track method is superior to standard neutron activation analysis in all cases where it is desirable to obtain information on the spatial distribution of the elements. In this case, the sample should of course not be powdered. The method allows the determination of uranium contents down to the 10^{-3} ppb range over areas less than 10^{-6} cm^2, and is therefore suitable for determining very small quantities of uranium, e.g., in mineralogical samples. For Th the limit of detection is in the ppb range [33].

The nuclear track technique is used in such diversified areas as geological studies, cosmic ray studies, dating studies, studies of meteorites and lunar specimens, studies of the solar system origin, solar flare studies, geochemistry of the heavy elements and the search for super-heavy elements, to mention just a few in the context of this paper [34].

Fission-track dating of impact glasses, obsidians, tektites, apatites, zircons, etc., may well complement other dating methods; it is based on observing the fossil tracks from spontaneous fission of ^{238}U in the specimen itself, after etching with a suitable reagent [34]. If a similar sample is irradiated with thermal neutrons, after annealing of the fossil tracks by heating, 'fresh' tracks from neutron-induced fission of ^{235}U can be observed after etching. The 'fission-track age' can be calculated from the equation:

$$t = (P_s/P_i)n(\sigma_F I/\lambda_{SF})$$

where P_s and P_i = number of spontaneous and induced tracks per unit area, respectively; I = ratio of the natural isotopic abundances of ^{235}U to ^{238}U (= 0.0072/0.9927); σ_F = cross-section for the reaction $^{235}U(n, f)$ (= 577×10^{-24} cm^2); λ_{SF} = partial decay constant of ^{238}U for spontaneous fission (= 8.42×10^{-17} y^{-1}) [35]; and n = neutron dose (neutron cm^{-2}). This method of age determination assumes that the latent fossil tracks are conserved over the geological time. Evidence for a complex thermal history of the sample can be found by comparing the parameters of spontaneous and induced (fresh!) tracks (track length and/or pit diameter). If the sample has been reheated in geological times, both the mean track diameter and the track density P_s will be lowered, and t must be corrected [36]. The study of the thermal history of geological samples is a unique aspect of the fission track method.

Radiochemical Neutron Activation Analysis (RNAA)

This method is selected when the elements of interest cannot be determined with sufficient accuracy (or not at all) by INAA because of very low concentrations of a very small amount of sample or the presence of a significant background or other interference. The samples are usually decomposed with sodium peroxide fusion in a zirconium crucible, or with hydrofluoric acid (nitric, sulphuric and/or perchloric acid) mixtures, e.g., in a teflon-lined bomb. Attention should be paid to the fact that some minerals, e.g., accessory minerals rich in REE, are very resistant to HF-acid attack (see, e.g., ref. 37). The purpose is to separate chemically the REE as a group from other elements in the sample, usually after neutron irradiation, and to use the separated REE fraction for quantitative gamma-ray analysis. Inactive carrier is added to facilitate the separations; the carrier also enables the determination of any loss during the separation procedures, *i.e.* the determination of chemical yield, e.g., by reactivation, at least if complete isotopic mixing has been achieved.

RNAA procedures for the separation of the individual REE have been described, e.g., ref. 38, but the technical capabilities of modern gamma-ray detectors should remove the need for such operations in most cases.

Numerous relatively fast procedures exist for separating the REE as a group from interfering activities [37, 39–42], based on a fluoride–hydroxide precipitation cycle, oxalate precipitation, ion exchange, adsorption on preformed precipitates, solvent extraction, etc. The group separation scheme of Smet *et al.* [37] is shown in Fig. 1.

The increased sensitivity of RNAA can be illustrated with results for the REE in ultrabasic rocks, shown in Table VI. Although often no data are obtained for Gd, Tb and Dy, a relatively smooth chondrite-normalized curve can be drawn as a function of atomic number, suggesting internal consistency of the data obtained (Fig. 2).

Boynton [43] reported new radiochemical neutron activation techniques permitting studies of microgram samples, but the analyses appear to be very painstaking, e.g., individual mineral grains are extracted from thin sections so that their petrogenetic setting can be found.

To summarize: neutron activation is a very specific and sensitive technique, which can mostly be purely instrumental. Simultaneous determination of many elements is possible, in particular of the REE, for which the technique is widely used in geochemical research laboratories. The cost for neutron irradiations would be high if they were to be obtained on a purely commercial basis. The cost of equipment for gamma-ray analysis varies considerably but is generally less than that of a mass-spectrometric facility.

Mass Spectrometric Analysis

Thermal Ionisation Isotope Dilution Mass Spectrometry (ID–MS)

This method is based on the mass spectrometric determination of the isotopic composition of an element. It is applicable to ten of the REE, including those which are of particular geochemical interest. The method is accurate and sensitive, seldom requiring more than 50–100 mg of material for a complete analysis; therefore, it is also suitable for separated minerals. These characteristics explain the very prominent role which the technique has played in the development of REE geochemistry, as exemplified by the work of Gast [44], Schnetzler and Philpotts [45], Kay and Gast [46], O'nions and Gronvold [47] and Arth and Hanson [48]. These papers generally give only minimal information on the analytical proce-

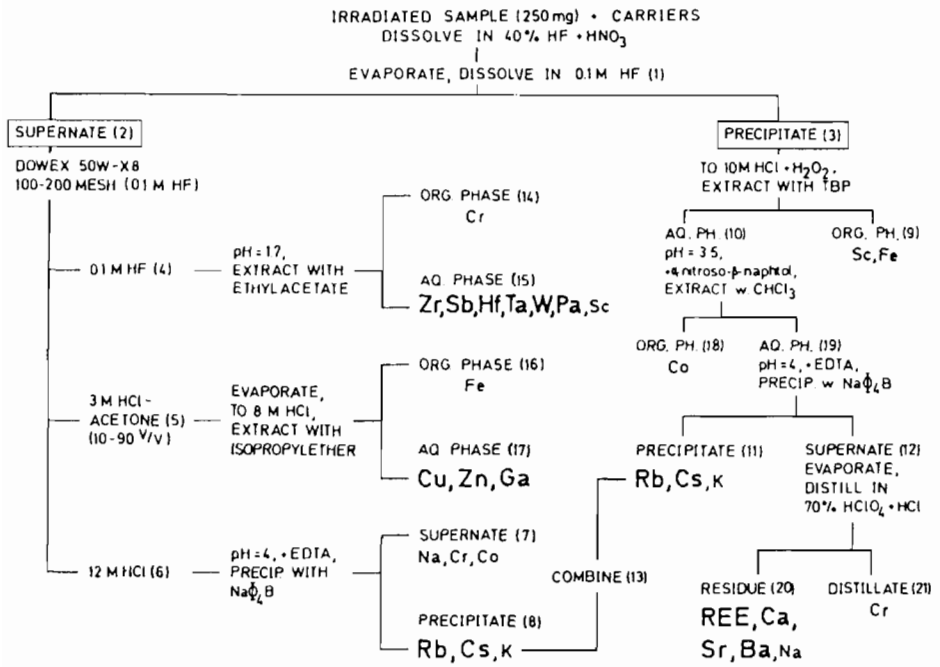

Fig. 1. Group separation scheme of Smet *et al.* [37]. Elements determined in each fraction are printed in boldface; the interfering elements are printed in small type.

TABLE VI. Determination of REE in Ultrabasic Rocks by RNAA Using the Group Separation Scheme of Smet *et al.* [37]

Element	Dunite DTS-1		Periodite PCC-1		Dunite NIM-D	
	Smet [37]	Flanagan [15]	Smet [37]	Flanagan [15]	Smet [37]	Flanagan [15]
La	0.022 ± 0.001	(0.04)	0.032 ± 0.002	0.15	0.082 ± 0.004	<3
Ce	0.059 ± 0.008	(0.06)	0.092 ± 0.005	0.09	0.164 ± 0.008	<10
Nd	0.028 ± 0.004	<0.02	0.023 ± 0.012		0.079 ± 0.006	
Sm	0.0041 ± 0.0002	(0.004)	0.0054 ± 0.0003	0.008	0.0110 ± 0.0005	
Eu	0.00093 ± 0.00006	0.0009	0.0012 ± 0.0001	0.002	0.0027 ± 0.0001	0.006
Tb					0.0030 ± 0.002	
Ho	<0.0009	(0.003)	<0.002		0.004 ± 0.001	
Tm	0.0012 ± 0.0006	(0.001)	0.0025 ± 0.0012		0.0045 ± 0.0008	
Yb	0.0108 ± 0.0005	(0.01)	0.025 ± 0.001	0.02	0.047 ± 0.002	<3
Lu	0.0022 ± 0.0001	(0.002)	0.0055 ± 0.003	(0.006)	0.0104 ± 0.0005	

All values are in ppm (weighted average of 2–3 determinations); uncertainty at 95% confidence interval.

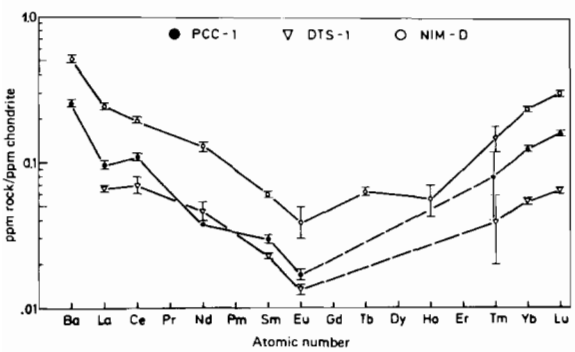

Fig. 2. Chondrite normalized Ba-REE curves for international standard rocks PCC-1, DTS-1 and NIM-D, obtained by RNAA [37].

dure. A general treatment on isotope dilution mass spectrometry was recently given by Heumann [49], and a detailed discussion with regard to the REE has been presented by Henderson and Pankhurst [50].

To the powdered rock sample, containing the REE in their natural isotopic abundance, isotopically enriched 'spikes' are added (obtained from Oak Ridge, U.S.A., or Harwell, U.K., for instance). Recommended spike and reference isotopes are indicated in Table VII [49]. Isotopic exchange must be ensured during and/or after dissolution of the rock powder, which is usually accomplished in a PTFE pressure vessel.

Chemical treatment of the solution (which needs not be quantitative) once the sample is completely

TABLE VII. Recommended Spike and Reference Isotopes of the Lanthanides, U and Th [49]

Element	Reference isotope				Spike isotope			
	Mass number	Natural abundance (%)	Half-life (years)	Interfering element	Mass number	Natural abundance (%)	Half-life (years)	Interfering element
La	139	99.91			138	0.09	1.4×10^{11}	Ba, Ce
Ce	140	88.48			142	11.08		Nd
Pr	141	100						
Pm								
Sm	152	26.7		Gd	149	13.8		
Eu	153	52.5			151	47.8		
Gd	157	15.65			155	14.8		
Tb	159	100						
Dy	163	24.9			161	18.9		
Ho	165	100						
Er	166	33.6			167	22.95		
Tm	169	100						
Yb	174	31.8		Hf	173	16.12		
Lu	175	97.41			176	2.59	3.6×10^{10}	Yb, Hf
Th	232	~100	1.4×10^{10}		230	10^{-4}	7.5×10^{4}	
U	238	99.2745	4.5×10^{9}		235	0.7200	7×10^{8}	

dissolved and isotopic equilibrium obtained, usually involves ion-exchange separations, e.g., on a cation-resin, such as Dowex-50, in HCl or HNO_3 medium. One of the simplest methods used is to elute with 2.5 M HCl until Sr is removed and then to collect two successive fractions in 6.2 M HCl, the first enriched in the heavy REE (HREE) and the second in the light ones (LREE) [51]. Alternative separation methods, e.g., yielding three fractions (HREE, MREE and LREE; *i.e.*, Dy–Lu, Nd–Gd, La–Ce) have been reviewed by Henderson and Pankhurst [50].

The separate REE fractions are loaded directly on a Ta, Re, W or other high-melting point filament as a drop which is taken to dryness. Singly charged ions are generated from the element of interest in a suitable ion source by thermal evaporation from the glowing filament. After acceleration the ions are usually separated in a magnetic analyser.

Evaporation and ionization can be obtained in one step by heating the filament to temperatures above 1000 °C ('single-filament ionization'). A more efficient though less convenient technique is to use a separate high-temperature ionization filament, while the sample is evaporated at a lower temperature from one or two side filaments ('double' or 'triple' filament ionizations). Triple filament ionization is essential for the analysis of all REE using one filament loading, as described by Thirlwall [52].

Measurement of the isotopic composition of the element after mixing with a known amount of the spike allows calculation of the element's concentration in the original sample. Ideally, isotope ratios can be measured with a precision of 0.1% or better. Uncertainties concerning mass fractionation during ionization and occasionally unidentified isobaric interferences (e.g., from multiply charged or complex ions, including MCl^+ and even hydrocarbons) sometimes degrade the accuracy of the measurement to 0.25–0.50%. Allowing for the propagation of errors from the spike calibration procedure, it is still reasonable to predict an overall accuracy better than 1%, except in unfavourable circumstances [50]. Results reported by Armstrong and Verbeek [53] for U.S. Geological Survey standard rock basalt BCR-1 are shown in Table VIII.

The chief disadvantages of the method are not only the need for expensive equipment and skilled operators, but also the time and effort required. For these reasons it is probable that as new, rapid and accurate analytical methods are developed (e.g., ICP–MS), the above described ID–MS will be reserved for cases especially requiring its high accuracy and sensitivity, as well as for calibration of other methods.

Compared to significantly more expensive magnetic sector instruments, thermionic quadrupole mass spectrometers, which are commercially available [54], produce analytical results of nearly the same quality at less expense and greater operating convenience, especially when considering that for ID–MS it is not the mass spectrometer (and therefore not the isotope ratio measurement) that is the limiting factor with respect to the precision of analysis results, but rather the chemical treatment of the sample, the blank problem and the sample inhomogeneity.

Different elements are emitted from the filament at different temperatures, so that elements can be

TABLE VIII. Comparison of Analysis with High Precision and Accuracy of Geological Standard USGS BCR-1 by Four Different Laboratories (values listed are in $\mu g\ g^{-1}$)

	Thermionic ID–MS [53]	ID–SSMS		ID-SSMS detection [63]		SSMS[a] [69]	Best estimate of true values [69]
		[68]	[69]	Photoplate	Electrical		
Ce	54.3	49.9	56.4	58.7	53.6	53.6	53.7
Nd	29.4	30.5	30.2	30.0	27.8	29.3	28.5
Sm	6.80	6.99	6.90	6.73	6.79	6.44	6.70
Eu	2.00	2.02	1.89	2.13	1.97	2.01	1.95
Gd	6.79	6.56	6.46	6.17	6.38	6.25	6.55
Dy	6.55	6.21	6.50	6.00	6.40	6.44	6.39
Er	3.74	3.67	3.98	3.33	3.80	3.73	3.70
Yb	3.50	3.30	3.32	3.32	3.49	3.69	3.48
Overall precision r.s.d. (%)	0.5	2.8 7.3 (Ce, Er)		6.5	2.7	4.6	

[a]Average of seven determinations by five analysts.

analysed sequentially in the presence of interfering ions, by gradually raising the filament temperature. Nevertheless, some interferences are unavoidable. For a detailed discussion, reference is made to Henderson and Pankhurst [50].

Recently, use is being made of resonance ionization mass spectrometry (RIMS) to eliminate or minimize isobaric interferences for the REE, without the need for chemical separation (e.g., Nd and Sm, Lu and Yb [55]; and for the actinides, e.g., Pu and U [56] by photoionizing selectively only one of two isobaric elemental species evaporated from a heated metal filament, using a dye-laser at a suitable wavelength. Provided that the laser power density is sufficiently high, ionization will occur for all atoms of that element within the laser volume; the resonance ionization effect will thus be saturated. The sensitivity is not as good as in conventional (pulse-counting) mass spectrometers if the duty cycle of the laser is too low.

Young *et al.* [57] have observed that there are many more RIMS-active transitions for Eu than would be expected for ground state Eu atoms. It was assumed that this observation demonstrated a more general phenomenon; if so, there is a possibility of more spectral interferences in RIMS than had been originally thought.

Spark Source Mass Spectrometry (SSMS)

In this method, the sample to be analysed should be in the form of conducting electrodes, between which high voltage radio frequency spark breakdowns are created in a vacuum. The positive ions produced are accelerated up to 20–30 kV, and mass analysed after energy filtering in a double focusing Mattauch–Herzog mass spectrometer. The technique is fully covered in a monograph [58], and an up-to-date review on the underlying physical principles and on applications has been given by Ramendik *et al.* [59]. The Mattauch–Herzog geometry enables the simultaneous detection of all elements from Li to U on an ion-sensitive emulsion at a mass resolution of typically 5000, but electrical detection (more precise but limited to a lower mass resolution) is also possible, e.g., by the magnetic peak switching mode.

In the absence of mass spectral interferences (e.g., from multiply charged ions or complex cluster ions) sensitivities are in the sub-ppm range; for ultrapure materials and long exposures, the sensitivities can increase to the 10 ppb level. Even without standards, semiquantitative results can be obtained because of the relatively uniform sensitivity factors.

Insulating samples, such as geological materials, are powdered and mixed with a high-purity conductor, such as graphite, aluminium or gold powder, pressed into electrodes and sparked; see ref. 60 and refs. given there for the determination of the lanthanides.

The application of isotope dilution to SSMS has considerably increased the reliability of the results. ID-SSMS was pioneered by Leipziger [61] and since that time it has also been used for geological samples [62–65]. Three different approaches of sample preparation have been described.

(a) Spiked graphite method: the samples are mechanically mixed with a previously spiked graphite [62]; isotopic exchange occurs during sparking.

(b) Sample dissolution method in a Teflon bomb in the presence of spikes (which improves the precision for inhomogeneous samples): the samples are converted to nitrates or oxides and the residue is mixed with ultrapure graphite [65].

(c) Group separation method: detection limits are improved, sample inhomogeneity problems are

avoided and interferences from major rock-forming elements are minimized by separation (preconcentration) of the REE as one or two groups (HREE and LREE), after sample dissolution in the presence of isotopically enriched spikes [63]. Several separation schemes have been used, e.g., cation exchange chromatography [66] or mixed-solvent anion exchange chromatography [67]. Using electrical detection, a precision of ±2 to ±4% was obtained by Van Puymbroeck and Gijbels [63]; Jochum recently reported even ±0.3 to ±1% [65]. Some results are shown in Table VIII and illustrate that ID–SSMS can give quite reliable results for lanthanides in silicate rocks.

Inductively Coupled Plasma Mass Spectrometry (ICP–MS)

ICP–MS is a combination of two established analytical techniques, combining the ease of sample introduction of the ICP with the high detecting power of the mass spectrometer. Samples are normally introduced to the ICP by the direct nebulisation of aqueous solutions. The plasma itself is maintained at an effective temperature greater than 5000 K by a stabilized radio frequency generator. Under such conditions, the most predominant sample species in the plasma are singly charged ions, with formation probabilities of over 90% for most elements. Via a special interface, ions can be sampled directly from the hot plasma at atmospheric pressure, and transported through successive pumping stages into a quadrupole mass filter at high vacuum, for mass analysis. The entire mass range can be scanned in a fraction of a second; successive scans are stored and build up to form the final spectrum. Total acquisition times of a few minutes are typical, therefore high sample throughput is possible. The state of the art has been described by Gray [70].

For the analysis of mineralogical samples, ICP–AES (atomic emission spectroscopy) is adequate in many cases, but particularly for the heavier elements, mass spectrometry has considerable advantages because of the greatly reduced interference problems associated with the simpler spectra. This is especially true for the REE. They may be analysed by emission spectrometry using a high resolution instrument, but the method is time consuming. ICP–AES interfaced with high performance liquid chromatography (HPLC) has been applied to the determination of REE, e.g., in rocks and ores, but also in high-purity REE oxides and chlorides [71].

Every REE has at least one interference-free isotope, whereas most of the more common members of the group have two or three isotopes free from isobaric interference and are therefore suitable for isotope dilution ICP–MS.

According to Gray [70] multi-element detection limits on REE, using the 3σ definition, are from less than 0.1 ng ml^{-1} for the monoisotopic REE to *ca.* 0.5 ng ml^{-1}. A spectrum of the Canadian Geological Survey standard silicate Syenite SY-3 in solution at 1 g in 100 ml is shown in Fig. 3. Results of a quantitative analysis of granite NIM-G are shown in Table IX together with other data for comparison. The ICP–

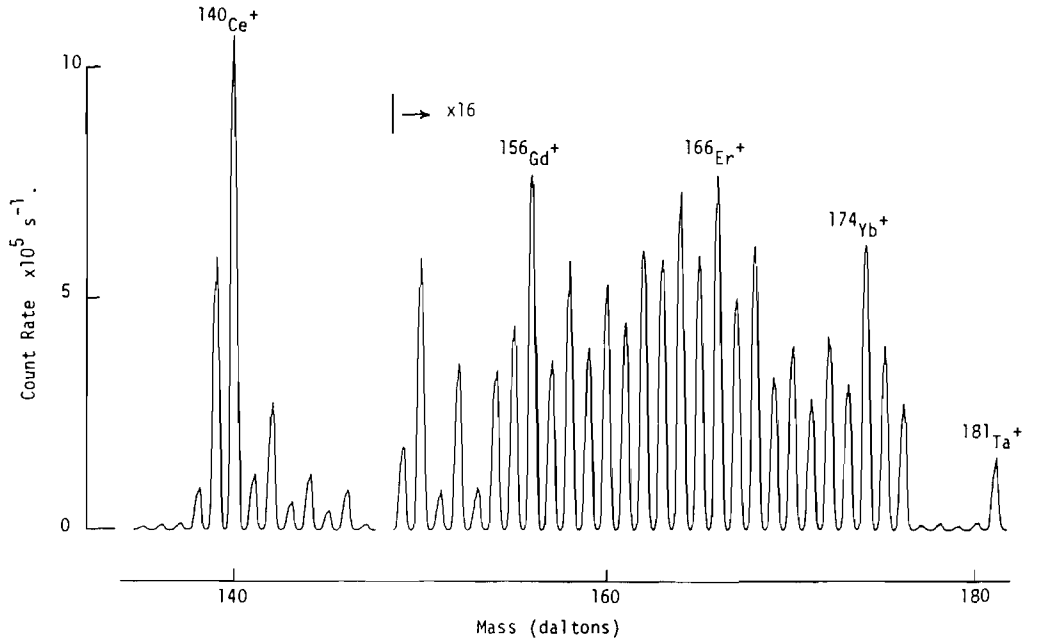

Fig. 3. REE spectrum obtained for international standard rock syenite SY-3 by ICP–MS in solution at 1.0 g in 100 ml [72].

TABLE IX. REE Data (in $\mu g\ g^{-1}$) for International Standard Reference Silicate Rock NIM-G (Granite)

Element	Ion used for ICP–MS	ICP–MS [72]	SSMS[a] [66]	Abbey [73]
La	$^{139}La^+$	110	105	105
Ce	$^{140}Ce^+$	200	195	200
Pr	$^{141}Pr^+$	21	18.9	
Nd	$^{146}Nd^+$	69	73	68
Sm	$^{147}Sm^+$	12	15.5	16
Eu	$^{153}Eu^+$	0.3	0.39	0.4
Gd	$^{157}Gd^+$	15	10.9	11
Tb	$^{159}Tb^+$	2.3	2.1	3
Dy	$^{163}Dy^+$	17	15.8	15
Ho	$^{165}Ho^+$	3.6	3.3	3
Er	$^{166}Er^+$	11	10.0	10
Tm	$^{169}Tm^+$	1.8	1.65	2
Yb	$^{172}Yb^+$	11	13.3	14
Lu	$^{175}Lu^+$	1.7	2.1	2

[a]After acid digestion of the rock and group separation of the REE by cation-exchange chromatography.

MS data were obtained from a single 1 min integration in each case for a blank solution in 1% HNO_3, a reference standard solution containing each REE at 1 $\mu g\ ml^{-1}$ in 1% HNO_3 and the sample solutions. Except for silica, which was removed during dissolution in HF, the matrix elements are present in solution. The agreement with accepted values is excellent for such a rapid analysis.

Conventionally, the analysis of impurities in uranium for the nuclear industry is undertaken by optical emission spectrometry. This technique suffers from the limitations of intrinsic lack of sensitivity, coupled with the fact that the complex uranium matrix spectrum obscures many relevant data. As a consequence, the uranium has to be removed by time-consuming extraction procedures [74]. The use of ICP–MS avoids the need for extensive sample pretreatment, as the uranium mass spectrum is very simple [75].

Secondary Ion Mass Spectrometry (SIMS) and in situ Microanalysis

In situ chemical analysis of localized areas in a polished thin or thick section, or in an individual mineral grain is usually accomplished by electron probe X-ray microanalysis (EPXMA), e.g. ref. 76. This technique is, however, not suitable for the determination of REE in most cases, because of insufficient sensitivity (detection limit ~500 ppm), not to mention the considerable overlap of the REE L series X-ray lines which are observed when analysing REE-rich minerals.

Proton-induced X-ray analysis offers some promise because of a better signal-to-background (Bremsstrahlung) ratio [77]; so far, only Ce and Nd concentrations at the 100 ppm level have been reported [78].

Potentially more sensitive is an X-ray fluorescence technique using synchroton radiation [79], based on the analysis of the K X-ray spectra of the REE. Detection limits on the order of 1 ppm are expected for the REE, but so far, no data have been reported for geological materials.

Most of the *in situ* measurements so far have been obtained by applying ion probe techniques. In this method, a beam of ions of a few KeV is directed towards the sample to be analysed. In order to minimize sample charging in insulating minerals, a beam of O^- ions is mostly used and the specimen is coated with a thin layer of gold. During the sputtering process, secondary particles are liberated from the sample surface, part of them as positive or negative ions, which can be mass spectrometrically analysed. By focusing the beam, one obtains an ion microprobe mass analyser, but even when using a broad beam (e.g., 300 μm in diameter) information on the lateral distribution of elements can be obtained with a suitable ion-optical system (ion microscope). Some commercial instruments combine both operation modes [80, 81]. Secondary ion mass spectrometry is very comprehensively covered in a recent monograph [82] and review [83]. Geological applications have been reviewed by Lovering [84], who hailed the ion microprobe the 'ultimate weapon' of the geochemist, by Shimizu *et al.* [85], Reed [86] and Crozaz and Zinner [87].

In principle, it is possible to detect certain elements at very low concentrations (a few ppb), but there are a number of limitations: while a spatial resolution of less than 0.1 μm can be obtained [88] and a depth resolution of ~0.01 μm (although this aspect is usually of no concern in geological applications), low limits of detection require larger spots and sampling accumulation over larger depths.

A very important limitation is the occurrence of many mass spectral interferences. The main interferences for REE atomic peaks are complex molecular ions formed from the major elements (e.g., CaP_2O_3, CaP_3O, $CaPO_5$, etc. in the case of a calcium phosphate), and oxides and hydroxides of the LREE at the masses of the HREE; occasionally also fluorides and even hydrides [86, 89]. This phenomenon also occurs in other mass spectrometric techniques, e.g., laser [90, 91] and even spark source mass spectrometry [63, 91]. Separation of the LREE oxides from the HREE atomic ions requires a mass resolving power $M/\Delta M$ of between 7000 and 9000, which can be obtained at the expense of sensitivity in modern commercial equipment, such as the Cameca IMS 3F and 4F ion microanalysers, based on a double focusing design [80, 81]. Figure 4 shows a SIMS spectrum from spencite [89], a natural REE-rich borosilicate, containing 12% H_2O, recorded at

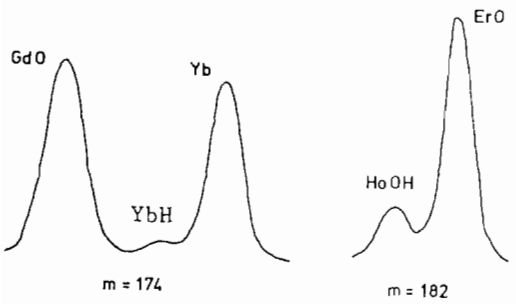

Fig. 4. Secondary ion mass spectrum from spencite [89] recorded at very high mass resolution using the 'SHRIMP' instrument [92].

very high mass resolution (>25 000) using the 'Sensitive High Resolution Ion Micro Probe (SHRIMP)' developed at the Australian National University [92]; hydride and hydroxide interferences at $m/z = 174$ and 182 are shown in this somewhat unusual case.

Another approach, which also results in the loss of sensitivity, but which is more convenient to use in practice, is the application (at low mass resolution) of energy filtering (*i.e.*, measuring high-energy secondary ions) to suppress molecular ions, whose energies are lower than those of atomic ions. This can be achieved by the specimen isolation technique (e.g. ref. 93) or by the conventional way, as described by Shimizu *et al.* [85] and by Zinner and Crozaz [94].

The specimen isolation technique appears to have a lower loss of sensitivity, and ion intensities are adequate for the detection of all the REE at the 100 ppb level [95]. Figure 5 shows a SIMS spectrum of a zircon by this technique [93]: oxides of the HREE are hardly visible, demonstrating the molecular ion suppression. A drawback of the specimen isolation technique is that the primary beam cannot be focused into a spot smaller than 50–100 μm while maintaining the charging conditions necessary for the energy selection effect. Moreover, sample charging depends on specimen conductivity and primary current density, and cannot well be controlled, creating a problem for quantitative analysis.

Zinner and Crozaz [94] recently proposed the use of a modest degree of energy filtering, by imposing a *ca.* 80 eV offset, using a Cameca IMS 3F ion probe [80]. Secondary ions are counted at the isotopic masses of major and trace elements of interest as well as in the mass range of the REE and REE monoxides (m/z from 133 to 191). Although complex molecular ions are removed effectively by the energy filtering, the remaining monoxide interferences have to be eliminated by deconvolution of the mass spectrum into contributions from the REE and their monoxides only; fluorides can also contribute and have to be corrected for.

In the early work on REE, it was assumed that all the REE had the same (albeit not well known) ion yield [85, 97], but in reality there are differences in relative sensitivities, which are also matrix dependent [98].

The use of standards, with uniform, known REE concentrations and the same major element composition as the sample to be analysed, is presently the

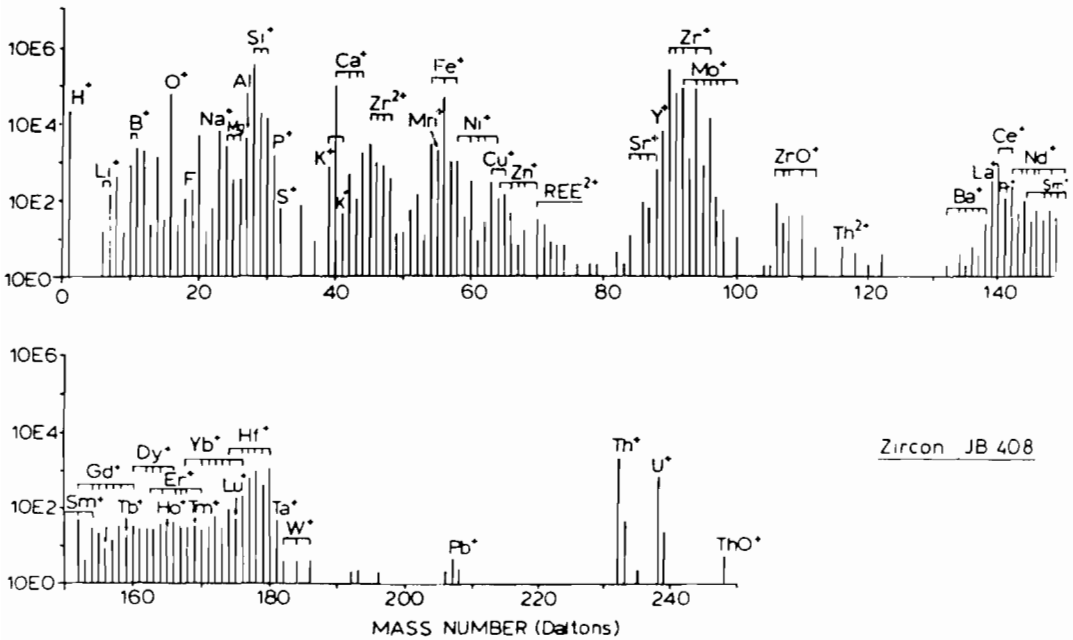

Fig. 5. Secondary ion mass spectrum ('bar graph') of a zircon crystal [93]. The peaks at $m/z = 233$ and 239 do not represent hydrides but are due to the broad and non-centered 232 and 238 peaks, respectively.

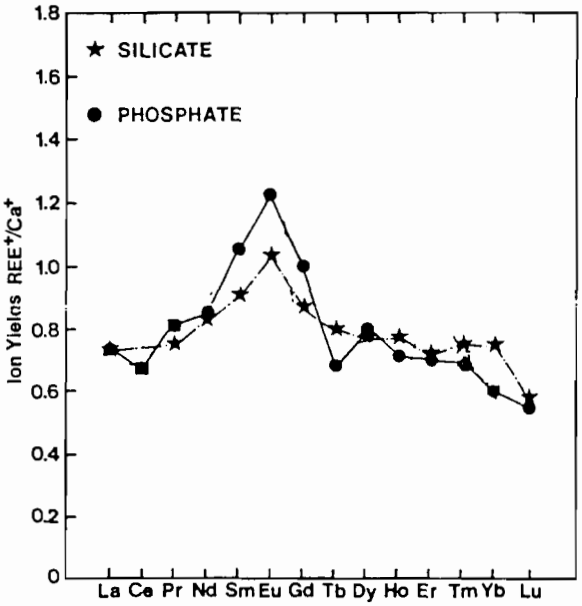

Fig. 6. Ion yields of the REE relative to Ca measured by SIMS with energy filtering in a silicate glass standard [99] and in a phosphate standard [94].

best way to convert relative ion intensities to elemental concentrations [87], but few such standards presently exist. Apatite samples, measured by other techniques such as neutron activation analysis or thermal ionization isotope dilution mass spectrometry, have been used successfully [98, 99]. By analysing silicates and phosphates, Crozaz and Zinner [87] found similar relative ion yields REE^+/Ca^+ in analysed silicates and phosphates, so that energy filtering not only removes interferences but also reduces matrix effects, see Fig. 6.

The ion probe techniques have progressed to the point where REE abundances in mineral grains can be determined not just in relatively REE-rich accessory phases, but also in relatively REE-poor major (silicate) phases. For a review on the existing literature, reference is made to Crozaz and Zinner [87].

References

1 L. A. Haskin and T. P. Paster, in K. A. Gschneider Jr. and L. Eyring (eds.), 'Handbook on the Physics and Chemistry of Rare Earths', North-Holland, Amsterdam, 1979, Chap. 21.
2 L. A. Haskin, F. A. Frey, R. A. Schmitt and R. H. Smith, in 'Physics and Chemistry of the Earth', Pergamon, Oxford, 1966, p. 167.
3 A. G. Herrmann, *Contrib. Mineral. Petrol., 17,* 275 (1968).
4 L. A. Haskin and R. L. Korotev, in 'Analysis and Application of Rare Earth Materials', *Proc. NATO Institute of Rare Earths Materials,* Institutt for Atomenergi, Kjeller, Norway, 23–29 August, 1972.
5 G. N. Hanson, *Ann. Rev. Earth Planet. Sci., 8,* 371 (1980).
6 P. Henderson (ed.), 'Rare Earth Element Geochemistry', Elsevier, Amsterdam, 1984, pp. 510.
7 J. Hertogen, in P. J. Elving, V. Krivan and I. M. Kolthoff (eds.), 'Treatise on Analytical Chemistry', Vol. 14, 2nd edn., Wiley, New York, 1986, p. 713.
8 L. A. Haskin and M. A. Gehl, *J. Geophys. Res., 67,* 2537 (1962).
9 L. A. Haskin, T. R. Wildeman and M. A. Haskin, *J. Radioanal. Chem., 1,* 337 (1968).
10 R. A. Schmitt, A. Mosen, C. S. Suffredini, J. E. Lasch, R. A. Scharp and D. A. Olehy, *Nature (London), 186,* 863 (1960).
11 G. E. Gordon, K. Randle, G. G. Goles, J. B. Corliss, M. H. Buson and S. S. Oxley, *Geochim. Cosmochim. Acta, 32,* 369 (1968).
12 J. Hertogen and R. Gijbels, *Anal. Chim. Acta, 56,* 61 (1971).
13 A. O. Brunfelt and E. Steinnes, *Anal. Chim. Acta, 48,* 13 (1969).
14 P. A. Baedecker, J. J. Rowe and E. Steinnes, *J. Radional. Chem., 40,* 115 (1977).
15 F. J. Flanagan, *Geochim. Cosmochim. Acta, 37,* 1189 (1973).
16 D. De Soete, R. Gijbels and J. Hoste, 'Neutron Activation Analysis', (Chemical Analysis Series, Vol. 34), Wiley–Interscience, New York, 1972.
17 R. Dams, F. De Corte, J. Hertogen, J. Hoste, W. Maenhaut and F. Adams, in T. S. West (ed.), 'Activation Analysis', Part 1, International Review of Science, Physical Chemistry, Series Two, Vol. 12, Analytical Chemistry, Part 1, Butterworths, London, 1976, p. 1.
18 J. C. Laul and L. A. Rancitelli, *J. Radional. Chem., 38,* 461 (1977).
19 R. Dybczynski, A. Tugsavul and O. Suschny, 'Report on the Intercomparison Run Soil-5 for the Determination of Trace Elements in Soil', IAEA/RL/46, Vienna, 1978.
20 S. Amiel, *Anal. Chem., 34,* 1683 (1962).
21 E. F. Dyer, J. F. Emery and G. W. Leddicotte, *USAEC Report ORNL-3342,* 1962.
22 N. H. Gale, 'Radioactive Dating and Methods for Low-level Counting', IAEA, Vienna, 1967, p. 431.
23 H. T. Millard Jr. and B. A. Keaten, *J. Radioanal. Chem., 72,* 489 (1982).
24 R. J. Rosenberg, V. Pitkanen and A. J. Sorsa, *J. Radional. Chem., 37,* 169 (1977).
25 N. N. Papadopoulos, *J. Radioanal. Chem., 72,* 463 (1982).
26 K. K. Bertine, L. H. Chan and K. K. Turekian, *Geochim. Cosmochim. Acta, 34,* 641 (1970).
27 B. S. Carpenter, *Anal. Chem., 44,* 600 (1972).
28 D. E. Fisher, *Anal. Chem., 42,* 414 (1970).
29 D. E. Fisher, *Geochim. Cosmochim. Acta, 34,* 630 (1970).
30 V. Murali, P. P. Parekh and M. Das Sanker, *Anal. Chim. Acta, 50,* 71 (1970).
31 W. G. Cross and L. Tommasino, *Proc. Symp. Clermont-Ferrand, Nuclear Track Registration in Insulating Solids and Applications, 1,* Clermont-Ferrand, France, 1969, p. 73.
32 D. R. Johnson, G. H. Bagett and K. Becker, *Health Phys., 18,* 424 (1970).
33 G. N. Flerov and I. G. Berzina, *J. Radioanal. Chem., 16,* 461 (1973).
34 R. L. Fleischer, P. B. Price and R. M. Walker, 'Nuclear Tracks in Solids, Principles and Applications', University of California Press, Berkeley, 1975, p. 605.
35 G. A. Wagner, G. M. Reimer, B. S. Carpenter, H. Faul, R. Van der Linden and R. Gijbels, *Geochim. Cosmochim. Acta, 39,* 1279 (1975).

36 D. Storzer, *Earth Planet. Sci. Lett., 8,* 55 (1970).
37 T. Smet, J. Hertogen, R. Gijbels and J. Hoste, *Anal. Chim. Acta, 101,* 45 (1978).
38 R. Becker, K. Buchtela, F. Grass, R. Kittl and G. Miller, *Z. Anal. Chem., 274,* 1 (1975).
39 J. Duffield and G. R. Gilmore, *J. Radioanal. Chem., 48,* 135 (1979).
40 R. Zilliacus, M. Kaistila and R. J. Rosenberg, *J. Radioanal. Chem., 71,* 323 (1982).
41 S. Meloni, M. Oddone, A. Cecchi and G. Poli, *J. Radioanal. Chem., 71,* 429 (1982).
42 E. B. Denechaud, P. A. Helmke and L. A. Haskin, *J. Radioanal. Chem., 6,* 97 (1970).
43 W. V. Boynton, in P. Henderson (ed.), 'Rare Earth Element Geochemistry', Elsevier, Amsterdam, 1984, pp. 63–114.
44 P. W. Gast, *Geochim. Cosmochim. Acta, 32,* 1057 (1968).
45 C. C. Schnetzler and J. A. Philpotts, *Geochim. Cosmochim. Acta, 34,* 331 (1970).
46 R. W. Kay and P. W. Gast, *J. Geol., 81,* 653 (1973).
47 R. K. O'nions and K. Gronvold, *Earth Planet. Sci. Lett., 19,* 397 (1973).
48 J. G. Arth and G. N. Hanson, *Geochim. Cosmochim. Acta, 39,* 325 (1975).
49 K. G. Heumann, in F. Adams, R. Gijbels and R. Van Grieken (eds.), 'Inorganic Mass Spectrometry' (Chemical Analysis Series), Wiley, New York, 1987, Chap. 8, in press.
50 P. Henderson and R. J. Pankhurst, in P. Henderson (ed.), 'Rare Earth Element Geochemistry', Elsevier, Amsterdam, 1984, pp. 467.
51 N. Shimizu, *Carnegie Inst. Washington, Yearbook, 73,* 941 (1974).
52 M. F. Thirlwall, *Chem. Geol., 35,* 155 (1982).
53 V. V. Armstrong and A. A. Verbeek, *S. Afr. J. Chem., 33,* 30 (1980).
54 K. G. Heumann, W. Schindlmeier, H. Zeininger and M. Schmidt, *Fresenius Z. Anal. Chem., 320,* 457 (1985).
55 D. L. Donohue, J. P. Young and D. H. Smith, *Int. J. Mass Spectrom. Ion Phys., 43,* 293 (1982).
56 D. L. Donohue, D. H. Smith, J. P. Young, H. S. McKown and C. A. Pritchard, *Anal. Chem., 56,* 379 (1984).
57 J. P. Young, D. L. Donohue and D. H. Smith, *Int. J. Mass Spectrom. Ion Proc., 56,* 307 (1984).
58 A. J. Ahearn (ed.), 'Trace Analysis by Mass Spectrometry', Academic Press, New York, 1972.
59 G. Ramendik, J. Verlinden and R. Gijbels, in F. Adams, R. Gijbels and R. Van Grieken (eds.), 'Inorganic Mass Spectrometry' (Chemical Analysis Series), Wiley, New York, 1987, in press.
60 J. Van Puymbroeck and R. Gijbels, *Bull. Soc. Chim. Belg., 87,* 803 (1978).
61 D. F. Leipziger, *Anal. Chem., 37,* 171 (1965).
62 J. F. Jaworski and G. H. Morrison, *Anal. Chem., 47,* 1173 (1975).
63 J. Van Puymbroeck and R. Gijbels, *Fresenius Z. Anal. Chem., 309,* 312 (1981).
64 K. P. Jochum, M. Seufert and F. Begemann, *Z. Naturforsch., Teil A, 35,* 57 (1980).
65 K. P. Jochum, in B. Sansoni (ed.), 'Instrumentelle Multielementanalyse', VCH Verlagsgesellschaft, Weinheim, F.R.G., 1985, p. 189.
66 F. W. E. Strelow and P. F. S. Jackson, *Anal. Chem., 46,* 1481 (1976).
67 P. J. Hooker, R. K. O'nions and R. J. Pankhurst, *Chem. Geol., 16,* 189 (1975).
68 K. P. Jochum, M. Seufert and H.-J. Knab, *Fresenius Z. Anal. Chem., 309,* 285 (1981).
69 H. E. Beske, R. Gijbels, A. Hurrle and K. P. Jochum, *Fresenius Z. Anal. Chem., 309,* 329 (1981).
70 A. L. Gray, in F. Adams, R. Gijbels and R. Van Grieken (eds.), 'Inorganic Mass Spectrometry' (Chemical Analysis Series), Wiley, New York, 1987, Chap. 7, in press.
71 K. Yoshida and H. Haraguchi, *Anal. Chem., 56,* 2580 (1984).
72 A. R. Date, unpublished results, quoted by A. L. Gray in ref. 70.
73 S. Abbey, *Geol. Survey Canada,* Papers 80–14 and 83–15.
74 P. S. Murty and R. M. Barnes, *J. Anal. Atomic Spectrom., 1,* 146 (1986).
75 P. D. Blair, *Trends Anal. Chem., 5,* 220 (1986).
76 S. J. B. Reed, 'Electron Microprobe Analysis', Cambridge University Press, Cambridge, 1975.
77 D. S. Burnett and D. S. Woolun, *Ann. Rev. Earth Planet. Sci., 11,* 329 (1983).
78 T. M. Benjamin, C. J. Duffy, C. J. Maggiore and P. S. Z. Rogers, *Nucl. Instr. Meth. Phys. Res., B, 3,* 677 (1984).
79 M. L. Rivers, I. M. Steele, J. V. Smith, A. L. Hanson, B. M. Gordon and K. W. Jones, *Trans. Am. Geophys. Union, EOS, 66,* 401 (1985).
80 M. Lepareur, *Rev. Tech. Thompson - CSF, 12,* 225 (1980).
81 H. N. Migeon, C. Le Pipec and J. J. Le Goux, in A. Benninghoven, R. J. Colton, D. S. Simons and H. W. Werner (eds.), 'Secondary Ion Mass Spectrometry, SIMS V', Springer-Verlag, Berlin, 1986, p. 155.
82 A. Benninghoven, F. G. Rüdenauer and H. W. Werner, 'Secondary Ion Mass Spectrometry: Basic Concepts, Instrumental Aspects, Applications and Trends' (Chemical Analysis Series, Vol. 86), Wiley, New York, 1987.
83 A. Lodding, in F. Adams, R. Gijbels and R. Van Grieken (eds.), 'Inorganic Mass Spectrometry' (Chemical Analysis Series), Wiley, New York, 1987, in press.
84 J. F. Lovering, *N.B.S. Spec. Publ., 427,* 135 (1975).
85 N. Shimizu, M. P. Semet and C. J. Allègre, *Geochim. Cosmochim. Acta, 42,* 1321 (1978).
86 S. J. B. Reed, *Scanning, 3,* 119 (1980).
87 G. Crozaz and E. Zinner, *Scanning Electron Microsc., 1986/II,* 369.
88 R. Levi-Setti, G. Crow and Y. C. Wang, *Scanning Electron Microsc., 1985/II,* 535.
89 S. J. B. Reed, *Scanning Electron Microsc., 1984/II,* 529.
90 E. Michiels, L. Van Vaeck and R. Gijbels, *Scanning Electron Microsc., 1984/III,* 1111.
91 S. Becker and H. J. Dietze, *ZfI-Mitt. (Leipzig), 101,* 61 (1985).
92 W. Compston, I. S. Williams and S. W. Clement, 'Proc. 30th Ann. Conf. Mass Spectrometry and Allied Topics, Honolulu, June 1982', Am. Soc. Mass Spectrom., 1982, p. 592.
93 J. B. Metson, G. M. Bancroft and H. W. Nesbitt, *Scanning Electron Microsc., 2,* 595 (1985).
94 E. Zinner and G. Crozaz, *Int. J. Mass Spectrom. Ion Proc., 69,* 17 (1986).
95 N. D. MacRae and J. B. Metson, *Chem. Geol., 53,* 325 (1985).
96 C. A. Andersen and J. R. Hinthorne, *Earth Planet. Sci. Lett., 14,* 195 (1972).
97 S. J. B. Reed, *Int. J. Mass Spectrom. Ion Phys., 54,* 31 (1983).
98 G. Crozaz and E. Zinner, *Meteoritics, 20,* 629 (1985).
99 E. Zinner and G. Crozaz, in A. Benninghoven, R. J. Colton, D. S. Simons and H. W. Werner (eds.), 'Secondary Ion Mass Spectrometry, SIMS V', Springer-Verlag, Berlin, 1986, p. 444.